Available online at www.sciencedirect.com
ScienceDirect
Journal of Nuclear Materials 362 (2007) 208–214
journal of nuclear materials
www.elsevier.com/locate/jnucmat

Development of multifilamentary niobium–titanium and niobium–tin strands for the International Thermonuclear Experimental Reactor project

L. Zhou [a,b], P.X. Zhang [a,b,*], X.D. Tang [b], X.H. Liu [b], Y.F. Lu [a], P.D. Weng [c], G. Grunblatt [d], Gia K. Hoang [d], C. Verwaerde [d]

[a] Northwest Institute for Nonferrous Metal Research, Xi'an, Shaanxi 710016, PR China
[b] Western Superconducting Technologies Co. Ltd., Xi'an, Shaanxi 710016, PR China
[c] Institute of Plasma Physics, Chinese Academy of Sciences, Hefei, PR China
[d] Alstom Magnets and Superconductors, 3 bis avenue Des trois Chenes, 90018 Belford Cedex, France

Abstract

The International Thermonuclear Experimental Reactor(ITER) device should demonstrate the scientific and technological possibility of commercial fusion energy production in large scale in order to solve the worldwide energy problem in the future. The superconducting magnet system is the key part of the ITER device to supply high magnetic fields for confining the deuterium–tritium plasma. The multifilament NbTi and Nb_3Sn strands with high quality have been studied to meet the specifications of superconducting strands for fabricating poloidal field coils (PF) and toroidal field coils (TF). For NbTi strands with 8306 filaments, J_c of 2910 A mm^{-2} (4.2 K, 5 T, 0.1 μV cm^{-1}) has been obtained by a conventional process. The proposed process could be used for fabrication of long strands with a unit length more than 5000 m. By an internal tin process the multifilamentary Nb_3Sn strands with a diameter of 0.79 mm and a unit length longer than 5000 m have been successfully fabricated. The highest non-Cu *Jcn* (12 T, 4.2 K, 0.1 μV cm^{-1}) value of 1249 A mm^{-2} has been obtained. The *n*-value of Nb_3Sn strands is larger than 20 and the residual resistance ratio (RRR) value lies between 150 and 220. The formation of the Nb_3Sn superconducting phase together with the evolution of microstructure has been investigated by neutron diffraction and scanning electron microscopy. The results indicate that the properties of NbTi and Nb_3Sn strands have already met basically the specifications proposed by the ITER program.

PACS: 74.70.−b; 74.70.Ad; 81.40.Ef

1. Introduction

In the 1980's, the Intermagnetics General Corporation Advanced Superconductors (IGC-AS) cooperated with Lawrence Livermore National Laboratory (LLNL) to develop an internal-tin conductor for fusion magnets, specifically those envisioned

* Corresponding author. Address: Northwest Institute for Nonferrous Metal Research, Xi'an, Shaanxi 710016, PR China. Fax: +86 29 86224487.
E-mail address: pxzhang@c-nin.com (P.X. Zhang).

0022-3115/$ - see front matter © 2007 Elsevier B.V. All rights reserved.
doi:10.1016/j.jnucmat.2007.01.274

for the International Thermonuclear Experimental Reactor (ITER) [1]. Due to high performance parameters of the ITER magnet system, a new set of requirements was imposed for superconducting strands. The strand specifications require a high J_c together with low hysteresis loss for Nb_3Sn strands. For NbTi strands, a high J_c at 5 T and 4.2 K should be reached, moreover even an acceptable J_c at 6.5 K should be available.

To meet Nb_3Sn strand specifications, many methods, such as bronze process [2], internal Sn process [3], powder in tube (PIT) process [4] and modified jelly roll process (MJR) [5] etc., have been proposed for preparation of high performance superconducting Nb_3Sn wires. Only the bronze process and internal tin process, however, have become dominant for ITER because of their commercial potentials. In the 1970's, Northwest Institute for Nonferrous Metal Research (NIN), as the leading research group in low temperature superconductor (LTC) field in China, studied the Nb_3Sn superconductors by the bronze process. In 1982, cooperating with Centre National de la Recherche Scientifique (CNRS) in France, NIN successfully developed the 15.4 T-solenoid magnet using our Nb_3Sn multifilamentary cables [6]. Recently NIN has successfully fabricated Nb_3Sn strands by internal tin route with a high J_c larger than the target J_c of ITER.

Since the 1960's, NIN has been making efforts to explore the routes for obtaining high-J_c NbTi wires by the conventional alloying process and also by an artificial pinning centers (APC) process. In the 1980's NIN successfully achieved the high J_c of 3400 A mm^{-2} (4.2 K, 5 T) by the conventional process [7], which was the highest value at that time for NbTi wires. Very recently NIN has been devoted to producing high performance NbTi wires on an industrial scale, which can meet the specifications of the ITER.

2. Experimental

The Nb47wt%Ti alloy was produced via the technique of electric arc melting at Western Superconducting Technologies Co. Ltd (WST). Under optimal conditions, the main impurity content in the ingots did not exceed: $C < 0.01$; $N < 0.008$; $O < 0.04$; $Fe < 0.01$ wt.%. The NbTi multifilament strands were fabricated by the conventional composite process, where the billet was assembled, welded, evacuated, extruded, and drawn. Several sequences of thermo-mechanical treatments of the NbTi strands were performed to produce a fine dispersion of α-Ti precipitates for attaining high J_c values. The NbTi strands with a diameter of 0.73 mm were composed of 8306 filaments, 5 μm in diameter. The copper to superconductor ratio was 1.63. At the present time NbTi strands longer than 5000 m can be fabricated.

The internal tin process was employed to fabricate Nb_3Sn strands according to the specifications of ITER. The cross sectional view of Nb_3Sn strands is shown in Fig. 1. Nb rods were first put into Cu tubes for getting Cu/Nb composite rods, which were afterwards bundled, assembled and extruded into multifilamentary Cu/Nb tubes. Sn–Ti core rods with the Ti content of 2–3 wt.% were inserted into the central part of these Cu/Nb tubes and then cold-worked down to the desired shape and size of subelements for the next restack. These subelements were further reassembled into a final billet with a Ta barrier and a stabilizing Cu outer layer. The weight of billets with 19 subelements could reach 50 kg and the unit length of final strands with a strand diameter of 0.79 mm could be 3000–5000 m. The Nb filament thickness after the final cold-working was 5 μm. The ratio of Cu and non-Cu area is close to 1:1. Heat treatments for Nb_3Sn strands in vacuum or Ar atmosphere were divided into two stages of low-temperature treatment (<848 K) for diffusion

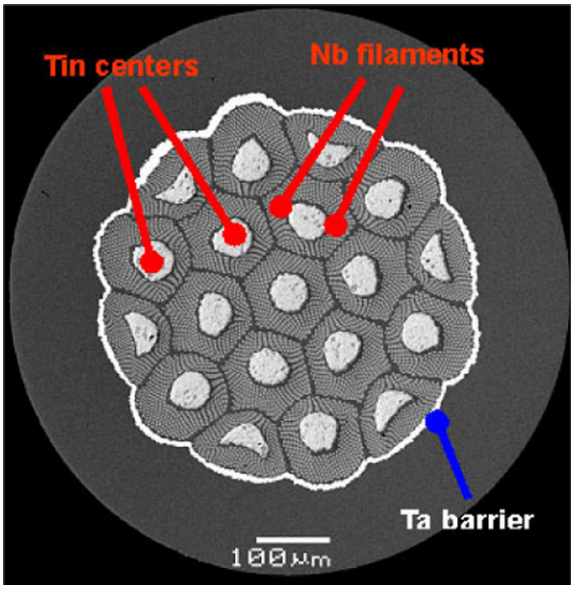

Fig. 1. The SEM cross-section of Nb_3Sn strand with ∅ 0.79 mm in diameter.

of Sn into Cu process and high-temperature treatment ($873 \sim 973$ K) for formation of superconducting Nb_3Sn phase through solid state diffusion. The total heat treatment time was about 350 h.

The critical current I_c of the strands was determined by a criterion of 0.1 μV cm^{-1} in different magnetic fields. The n-value was calculated as the slope of the log V–log I plot between 0.1 and 1.0 μV cm^{-1} using a least mean square fit. The critical temperature was measured by the standard four-probe method. The magnetization hysteresis loop was obtained at 4.2 K with magnetic field sweeping between +3 and −3 T. The microstructure of strands was investigated by a JEOL JSM-5410 scanning electron microscopy (SEM).

3. Results and discussion

For the NbTi strands with a Cu/non-Cu ratio of 1.63, the processing parameters were optimized for getting high J_c values, where four times of the thermo-mechanical treatments at 658 K for 40 h was done. Fig. 2 shows a representative $J_c(B)$ curve measured at 4.2 K for 8306-filamnet NbTi strands. The measured J_c has reached 2910 A mm^{-2} (4.2 K, 5 T, 0.1 μV cm^{-1}) higher than the specified value by ITER project. From critical current characteristics the n-values larger than 30 at 5 T have derived for the NbTi strands. In order to gain reliable electromagnetic behavior for different superconducting coils during ITER operation, an expected temperature margin $\Delta T = (T_{cs} - T_{op})$ has been proposed [8], where T_{cs} is the current sharing temperature and T_{op} the operating temperature. Recently, much attention has been therefore paid to the temperature dependence of critical currents for superconducting strands of ITER. The $I_c(T)$ curves in different applied fields have also been measured for NbTi strands (see Fig. 3). The scattered data are likely due to the instability of sample temperatures during current sweeping. The critical current has been found to decrease exponentially with increasing temperature and I_c is essentially zero when the temperature is close to 6 K for the investigated NbTi strand. This kind of $J_c(T)$ behavior does not agree with the temperature scaling law studied by Bottura [9], where a nearly linear $I_c$variation as a function of temperature was proposed. Two possibilities might be responsible for this behavior of $I_c(T)$. One is a mismatch between the readout of the sensor and the actual strand temperature. The other is related to the properties of the NbTi strand itself. New experiments are needed to find actual reasons and to further improve the $I_c(T)$ behavior in the future.

For the ITER Poloidal Field (PF) coils, NbTi strands with a higher Cu/non-Cu ratio (4.4 for PF5; 6.9 for PF2/3/4) are desired while a high J_c should be maintained according to the present design of ITER. These coils will be manufactured in China. Here it must be pointed out that for NbTi strands with a higher Cu/non-Cu ratio the working technique for long wires must be optimized, because the difference in the mechanical workability of NbTi alloy and Cu matrix might lead to non-homogenous deformation of strands and even filament breakage. The relevant research work is in progress now.

The Nb_3Sn strands were prepared by the internal tin route. It has been generally accepted that titanium as a third element introduced into Nb_3Sn can increase the upper critical field and lower the

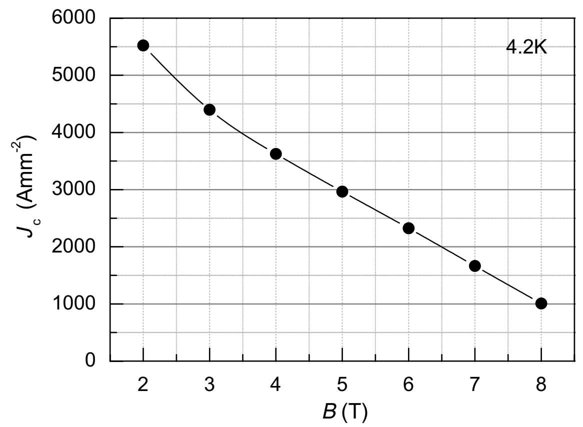

Fig. 2. The critical current density of NbTi strands at 4.2 K in different field.

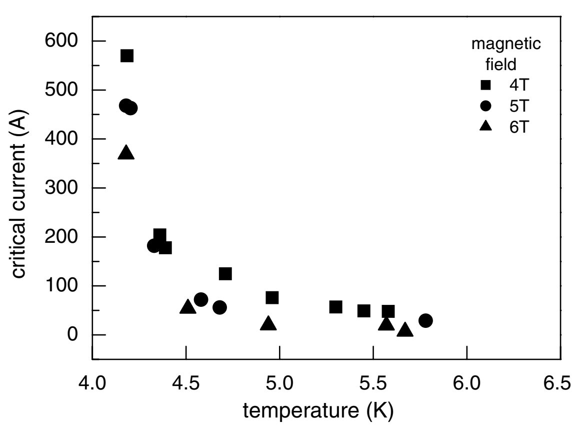

Fig. 3. $I_c(T)$ curves of NbTi strands for different magnetic fields.

critical current density at lower fields, thus reducing the losses [10]. Based on consideration from materials aspect, the introduction of Ti can speed up the diffusion of Sn and therefore improve the formation of superconducting Nb_3Sn phase in internal tin route [10]. Due to the diversity of conductor layouts in internal tin route, several different ways of Ti addition have been proposed and utilized in strand fabrications [10]. In our strands NIN has employed the method of alloying with Sn [11], that means, the Ti is included in the Sn core, where the Sn2-3%Ti alloy ingot was prepared by electron beam melting. Under optimal technical conditions, a dispersion distribution of rather fine intermetallic precipitates was obtained [12], resulting in an effective strengthening of Sn–Ti cores. During subsequent working processes the formation of Sn/Ti intermetallic compounds did not cause breakage in the fine filaments. Sn/Ti ingots with a high quality on a large scale can be fabricated.

In present paper the effects of heat treatment on phase formation, microstructures and superconducting properties are discussed for the optimal billet design of Nb_3Sn strands. The strands were treated by reaction heat treatment at temperatures from 848 to 973 K. Fig. 4 shows the results of the T_c measurements obtained on the samples under different heat treatments. The measurements were performed by a four-probe resistive method. The linear relationship between T_c and B was found to be kept for the samples treated at different temperatures and time. With increasing heat treatment temperature and time, the T_c shows a slight increase for Nb_3Sn strands, where the heat treatment temperature and time were was changed not so greatly. It has been generally believed that the T_c is inversely proportional to the lattice constant of Nb_3Sn compounds. The variation of the lattice constant is usually related to various factors: direct substitution effect of third-element, difference in the chemical stoichiometry, and lattice distortion during cold working as well. Although no lattice constant data were measured, the weak dependence of T_c on the heat treatment suggests that the chemical stoichiometry approaches the ideal one with increasing the heat treatment temperature if two samples of 898 K × 150 h and 923 K × 75 h are compared. With increasing the heat treatment time at 923 K the T_c continues to increase by a small amount, implying the Sn content still increases in the Nb_3Sn layers.

Fig. 5 indicates the non-Cu J_c at 4.2 K for the Nb_3Sn samples as a function of the magnetic field. The sample of 923 K × 150 h shows the best J_c value over the entire measured field range. It was tried to shorten the heat treatment time at relatively high temperature of 938 K for Nb_3Sn strands. The results showed that the heat treatment at higher temperature degraded the J_c at low field range very little. The heat treatment with short duration or at low temperatures even with a long duration had a negative effect on the J_c of Nb_3Sn strands. This can be attributed to the difference in the formation of superconducting phase and in the microstructure. This point will be discussed later. All samples above have J_c values higher than the target J_c of

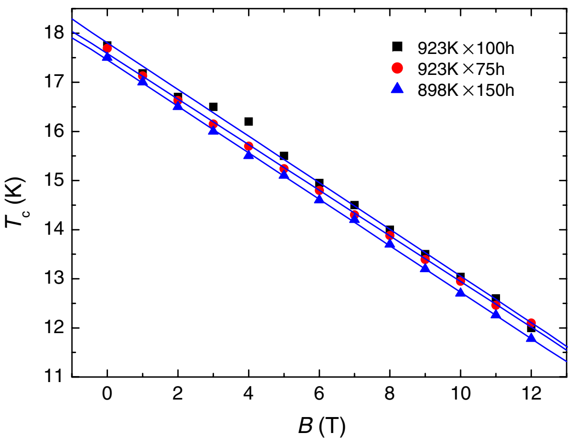

Fig. 4. $T_c(B)$ relationship of Nb_3Sn strands under different heat treatments.

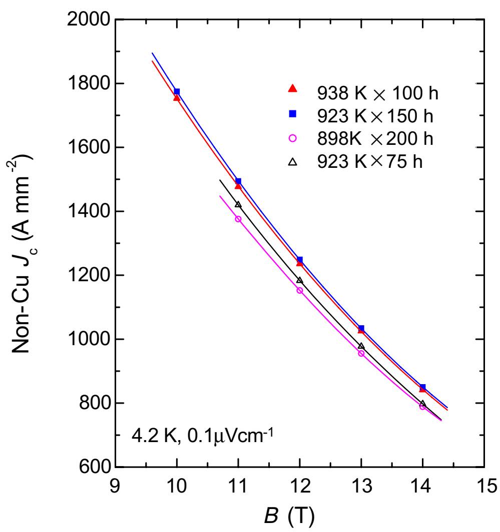

Fig. 5. Non-Cu J_c at 4.2 K for the Nb_3Sn samples as a function of the magnetic field.

1000 A mm^{-2} (4.2 K, 12 T) proposed by the ITER project. It should be pointed out that the magnitude of hysteresis loss for Nb_3Sn strands must be lower than the upper limit of 1000 mJ cm^{-3} (4.2 K, $\pm$3 T) for non-Cu area. It is rather challenging to attain not only high J_c but also low hysteresis loss for the ITER Nb_3Sn strands.

In order to find a relation between critical current density and microstructures SEM images are given for Nb_3Sn strands after reaction heat treatments as shown in Fig. 6. For the sample of 898 K $\times$ 200 h un-reacted Nb cores are visible (see Fig. 6a). As the heat treatment temperature was increased to 923 K, the fraction of un-reacted Nb cores obviously decreased. With further increasing heat treatment time un-reacted Nb cores were not detectable. The whole filaments are fully reacted into the superconducting Nb_3Sn phase. If the strands experienced a heat treatment of 938 K $\times$ 100 h (see Fig. 6d), the situation of the reacted Nb_3Sn phase was similar to that of 923 K $\times$ 150 h. Therefore, the lower values of J_c for the samples of 898 K $\times$ 200 h and 923 K $\times$ 75 h originated from a lower fraction of the Nb_3Sn phase due to the existence of not fully reacted Nb cores. The high J_c for two samples of 923 K $\times$ 150 h and 938 K $\times$ 100 h could be attributed to a larger fraction of the Nb_3Sn phase.

For Nb_3Sn superconductors, grain boundaries are believed to serve as the magnetic flux pinning centers. It is known that the pinning force density scales with inverse grain size. Reducing grain size and therefore increasing the density of grain boundaries are the main aim of mechanical working and heat treatment for Nb_3Sn strands. At lower heat treatment temperature, the growth of Nb_3Sn layers is dominant, while the grain growth is less important; at intermediate heat treatment temperature both effects play an important role in determining formation of Nb_3Sn phase and growth of grains. If the heat treatment was done at higher temperature, the growth of Nb_3Sn layers was finished within a short time but the grains continued to grow larger. In order compare the grain size the SEM micrographs are given for different heat treatments in Fig. 7. Average grain size of Nb_3Sn layers was estimated in parallel (parallel to the diffusion direction) and perpendicular directions. For the sample of 898 K $\times$ 200 h the average grain size was about 92 nm. With increasing heat treatment temperature the average grain size increased to 101 nm. On further increasing heat treatment temperature to 938 K, the enlargement of the grains was rather obvious (the average grain size 117 nm). Moreover, the dispersion of the grain size was relatively wide if compared to previous two samples. When the

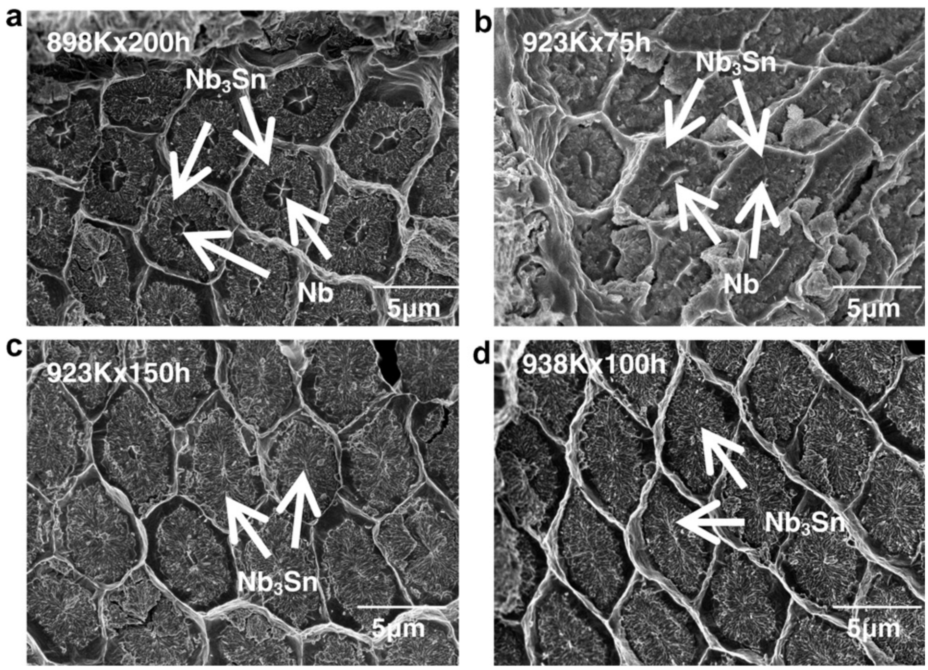

Fig. 6. SEM images of the central parts of strands after heat treatment. (a) Strands after 898 K/200 h; (b) strands after 923 K/75 h; (c) strands after 923 K/150 h; (d) strands after 938 K/100 h.

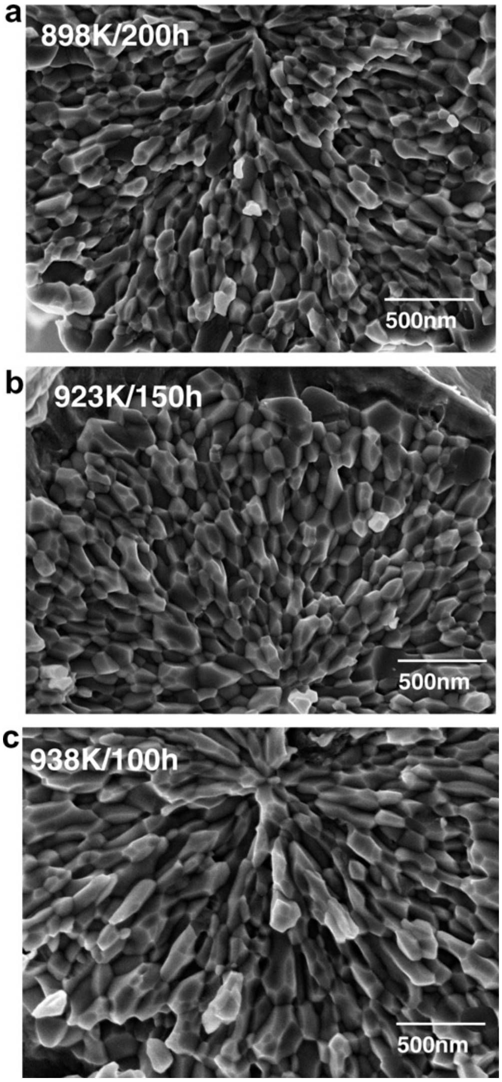

Fig. 7. Microstructure of Nb_3Sn grains in strands. (a) 98 K/200 h; (b) 23 K/150 h; (c) 38 K/100 h.

average grain size was correlated with the J_c values for these samples, it was found that within the chosen temperature range the fraction of Nb_3Sn was a dominant factor affecting the J_c of strands.

The hysteresis losses measured at 4.2 K based on a +/−3 T magnetization loop were compared for four samples in Fig. 5. The hysteresis losses were 750, 460, 1470 and 1441 mJ cm^{-3} for the samples of 898 K × 200 h, 923 K × 75 h, 923 K × 150 h, and 938 K × 100 h, respectively. According to the upper limit 1000 mJ cm^{-3} of hysteresis loss for ITER it was found that it was easy to attain this limit value if a relatively low heat treatment temperature was chosen with a shorter duration. Because the same billet design was used for four samples, the increase of hysteresis loss for two samples of 923 K × 150 h and 938 K × 100 h might originate from a volume change during the formation of more Nb_3Sn phase. This kind of the lattice volume increase may lead to higher possibility of element bridging, which is directly responsible for hysteresis losses in internal-tin Nb_3Sn strands. Achieving a low hysteresis loss is usually at the expense of reducing J_c by an acceptable amount. It is fortunate that there is much space for lowering J_c for these samples. Future work will concentrate on further refinements of strand layout to reduce the effective filament size down to smaller than 50 μm, while simultaneously increasing the critical current density of the Nb_3Sn layer itself through improving heat treatment routes.

The *n*-value is usually used as an indicator of the quality of practical superconductors. In multifilamentary wires any distribution of the properties of filaments, such as filament inhomogeneity and local critical current distribution, can give rise to variation of the *n*-value. The derived *n*-value from measured *V–I* curves can therefore reflect many properties related to strand design, strand working, and heat treatment for superconducting wires. The *n*-values of all strands measured at 4.2 K and 12 T were calculated. The magnetic field dependence of the *n*-value of some samples was estimated. The results have shown the *n*-value exceeds 20 specified by the ITER project for the samples subjected to heat treatments of (898–938) K × (100–200) h. The field dependence of the *n*-value has been mainly studied in the range from 10 to 14 T at 4.2 K for several samples. In most cases a good linear dependence of the *n*-value on magnetic field *B* was observed. The *n*-values of Nb_3Sn strands showed a normal decrease with the applied magnetic field, although the slope of *n–B* curves varied with the difference in strand layouts or heat treatments. This point may imply that an extrinsic effect such as filament sausaging is less important, because the lower dependence of n on magnetic field could be expected if the sausaging effect was dominant [13]. In Fig. 8, two representative *n–B* curves are plotted for the samples treated at 938 and 923 K. The sample treated at 938 K had a higher *n*-value than that for the sample treated at 923 K. Moreover, the slopes of the two *n–B* curves are different. The critical current density J_c, however, was actually the same for the two samples as shown in Fig. 5. The sample of 938 K × 100 h had greater standard deviation of grain size due to the faster growth of some

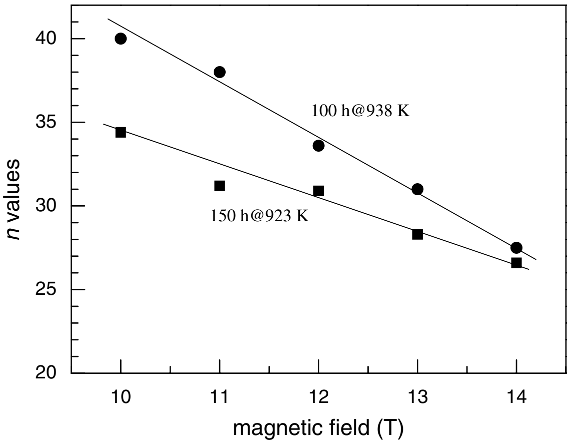

Fig. 8. *n*-*B* properties of Nb_3Sn strands treated at 938 and 923 K at 4.2 K.

grains if the heat treatment temperature was raised. If it is assumed that the distribution of grain size is related to the *n*-value, a lower *n*-value for larger standard deviation of grain size could be expected for the sample of 938 K × 100 h [14]. But the situation is opposite from the experiment. Therefore it is believed that the local chemical stoichiometry in the filaments for the sample of 938 K × 100 h is much more uniform, because raising heat treatment temperature speeds up the diffusion of Sn. It is possible that the stoichiometry in the Nb_3Sn layers is much more homogenous, resulting in a slightly higher B_{c2}, which is correlated with higher *n*-value [15]. The scaling law between critical current I_c and *n*-value for our strands will be reported elsewhere.

4. Conclusion

NbTi and Nb_3Sn superconducting strands have been produced from large-scale billets. The main technical specifications of the strands have achieved the requirement proposed by the ITER program. The weight of the billets can exceed 50 kg and the unit length of strands with high J_c was larger than 5000 m. The temperature dependent J_c properties for NbTi strands and the J_c-strain dependence for Nb_3Sn strands will be studied in the future.

Acknowledgement

This work was supported by the National Basic Research Program (973) in China with No. 2005CB724004.

References

[1] L.T. Summers, A.R. Duenas, C.E. Karlsen, G.M. Ozeryansky, E. Gregory, IEEE Trans. 27 (1991) 1763.
[2] A.R. Kaufmann, J.J. Picett, Bull. Am. Phys. Soc. 15 (1970) 838.
[3] Y. Hashimoto, K. Yoshizaki, M. Tanaka, Proc. 5th ICEC (1974) 332.
[4] J.D. Elen, C.A.M. van Beijnen, C.A.M. van der Klein, IEEE Trans. Magn., MAG-13 (1977) 470.
[5] W.K. McDonald, C.W. Curtis, R.M. Scanlan, D.C. Larbalestier, K. Marken, D.B. Smathers, IEEE Trans. Magn. MAG-19 (1983) 1124.
[6] L. Zhou et al., IEEE Trans. Mag. MAG-17 (1981) 2293.
[7] Zhou Lian, Li Chengren, Wu Xiaozu, et al., Journal de Physique. Colloque C1 (1984) 437.
[8] D. Bessette et al., IEEE Trans. Appl. Supercond. 11 (2001) 1550.
[9] L. Bottura, IEEE Trans. Appl. Supercond. 10 (2000) 1054.
[10] E. Gregory, M. Tomsic, M.D. Sumption, X. Peng, X. Wu, E.W. Collings, B.A. Zeitlin, IEEE Trans. Appl. Supercond. 15 (2005) 3478.
[11] M. Suenaga, C. Klamut, N. Higuchi, T. Kuroda, IEEE Trans. Magn. 21 (1985) 305.
[12] P.X. Zhang, L. Zhou, et al., Physica C 445–448 (2006) 819.
[13] W.H. Warnes, D.C. Larbalestier, Cryogenics 26 (1986) 643.
[14] A.E. Vorobieva, A.K. Shikov, V.I. Pantsyrny, E.A. Dergunova, K.A. Mareev, D.A. Farafonov, L.I. Vojdaev, V.M. Lonaev, IEEE Trans. Appl. Supercond. 15 (2005) 3407.
[15] T. Miyazaki, Y. Inoue, T. Miyatake, Y. Fukumoto, M. Shimada, IEEE Trans. Appl. Supercond. 5 (1995) 1781.